Research

Ewing sarcoma of the rib: respiratory tract infection as initial symptoms in a 14-year-old boy. Functional medical imaging findings

Angel González-Sistal[1] (angelgonzalez at ub dot edu) #, Alicia Baltasar-Sánchez[1], Miguel Garrido Pumar[2], Álvaro Ruibal Morell[2]
[1] Department of Physiological Sciences II, Faculty of Medicine. University of Barcelona. Spain. [2] Nuclear Medicine Service. Complejo Hospitalario Universitario. Santiago de Compostela. Spain

: corresponding author

DOI http://dx.doi.org/10.13070/rs.en.1.839
Date 2014-05-28
Cite as Research 2014;1:839

Abstract

Ewing sarcoma or primitive neuroectodermal tumor (PNET) of bone is the second most common pediatric malignant bone tumor. The median age at diagnosis is 15 years and there is a male predilection of 1.5/1. The authors present the case of a 14-year-old boy with Ewing sarcoma situated on the left ninth rib which was being investigated for respiratory tract infection. Pleurisy is the most common misdiagnosis. Our case illustrates the importance of recognizing exceptional features when interpreting FDG PET or scintigraphy to prevent the misinterpretation of metastases as other etiologies, such as infection.

INTRODUCTION

Ewing sarcoma or primitive neuroectodermal tumor (PNET) of bone is the second most common pediatric malignant bone tumor. The median age at diagnosis is 15 years and there is a male predilection of 1.5/1. PNET are high-grade tumors that usually metastasize to lungs, pleural spaces and bones. The prognosis of the patients changes significantly in the absence and presence of metastatic disease. Present algorithm workup includes: computed tomography (CT) scan of the chest to study skeletal metastasis, magnetic resonance imaging (MRI) for local tumor extent and Tc-99m whole-body scintigraphy to exclude skeletal metastasis. However, these techniques differ in performance in terms of sensitivity and specificity, but none of the modalities alone seem to be able to yield a reliable diagnostic outcome. FDG positron emission tomography (FDG PET) has the ability to image tumor glucose metabolism noninvasively. FDG uptake is regarded as a surrogate marker for the degree of tumor aggressiveness in many malignancies. Besides, FDG PET is an ideal method to assess tumor response. Presented is a case of Ewing sarcoma of the rib which illustrates the importance of recognizing exceptional features when interpreting FDG PET or scintigraphy to prevent the misinterpretation of metastases as perhaps other etiologies, such as infection.

CASE REPORT

[enlarge]

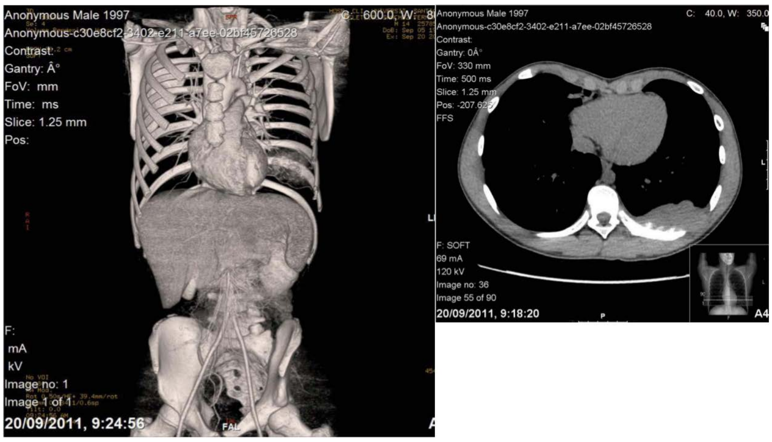

Figure 1. Computed tomography scan of the chest shows an expansive mass occupying the left hemithorax extending from the abnormal rib. Tumor was located over posterior arch of the left ninth rib.

A 14-year-old boy presented to the casualty department with localized left-sided chest pain and fever (August 2011). A plain chest x-ray showed an opacity in the base of the left lung. Patient was being investigated for pneumonia and treated with antibiotic during 10 days. Subsequently, the patient consulted the emergency ward about 2-days history of pain in the left hip which radiates to lumbar back and buttock, asthenia and fever. A plain pelvis x-ray was unremarkable. Patient was diagnosed of acute pharyngitis and treated. The patient came to the casualty department, for the third time, with left flank severe pain, not cough, not dyspnea, not nasal mucus and fever (38.6º). A plain chest x-ray showed a basal nodular opacity in the middle lobe of the lung and other left basal paracardiac opacity very suggestive of encapsulated pleural effusion which is an uncommon radiological finding in young patients with chest pain. Multimodal medical imaging studies evidenced a rib mass [1]. It was biopsied and Ewing's sarcoma was confirmed (September 2011). Functional medical imaging studies evidenced an additional lesion in the sacral bone.

[enlarge]

Figure 2. (A): Bone scintigraphy scan was requested to rule out multiple lesions. The images shows increased local tracer localization in the left ninth rib and it was discovered a new lesion in the left sacral alae. (B): Coronal PET shows an area of increased FDG uptake in the posterior arch of the left a maximum standard uptake value of 6.6.

A computed tomography (CT) (Fig. 1A, 1B) scan of the chest showed an expansive mass (80 x 45 x 60mm) occupying the left hemithorax extending from the abnormal rib. Tumor was located over posterior arch of the left ninth rib. A second mass of 35 x 30 x 34mm located to the right hemithorax, closed to right atrium, at pleural level was discovered. Bone scintigraphy (Fig. 2A) scan was requested to rule out multiple lesions. The images showed increased local tracer localization in the left ninth rib and it was discovered a new lesion in the left sacral alae.

[enlarge]

Figure 3. Follow-up imaging studies. (A): Coronal PET reveals a diffusing increased uptake in the bone marrow, without foci, as a result of reaction to postchemotherapy pancytopenia. (B): Scintigraphy does not show any bone alteration.

Wholebody PET (Fig. 2B), after injection of 171MBq of 18-F-FDG, showed an area of increased FDG uptake in the posterior arch of the left ninth rib with soft-tissue involvement measuring 20 x 53 x 64 mm with a Maximum Standard Uptakes Values (SUV_{max}) of 6.6, suggesting a malignant nature. PET confirmed an hypermetabolic homogeneous solid well-demarcated mass closed to right atrium 38 x 37 mm with an SUV_{max} of 12.4, suggesting a malignant nature. PET detected a little not well defined mass in the middle lobe of the rigth lung measuring 11mm (SUV_{max} 1.9), suggesting etiologies such as infection or inflammation. Increased FDG uptake in pelvis was seen numerous millimeter focus in the left sacroiliac bone (SUV_{max} 2.9), corresponding to the same pathological foci described on bone scintigraphy. A little abdominal focus localized in large bowel (cecum) suggested a benign process.

[enlarge]

Figure 4. Axial pelvic magnetic resonance imaging suggests bone necrosis in the left sacral alae.

Postchemotherapy 18-F-FDG PET (Fig. 3A) revealed a diffusing increased uptake in the bone marrow, without foci, as a result of reaction to postchemotherapy pancytopenia. The image showed a full disappearance of rib tumor focus and right lung focus. Findings indicate a favorable response to therapy. There was not hypermetabolic activity corresponding to other pathological foci. The sacroiliac bone was difficult to assess due to the diffusing increased uptake of FDG. Scintigraphy (Fig. 3B) did not show any bone alteration. Pelvic magnetic resonance imaging (MRI) (Fig. 4) suggesting bone necrosis in the left sacral alae. Restaging computed tomography scan (Fig. 5) obtained following chemotherapy and surgery showed a fibrotic scar in the posterior basal segment of the lung. The bronchiectasis in the right lung suggested an infective airways disease in resolution phase.

DISCUSSION

[enlarge]

Ewing sarcoma is preferentially located in the long bones or in the pelvis, the ribs being the third most frequent site (making up 10-15% of all cases) [2]. Ewing sarcoma is the most frequent chest wall tumor in children and adolescents [3]. Chest pain in children and adolescents leads to consideration of a number of differential diagnoses: musculoskeletal trauma, pneumothorax, pleurisy, myocarditis, pericarditis, respiratory infections, pleurodynia and bone malignancies [4].

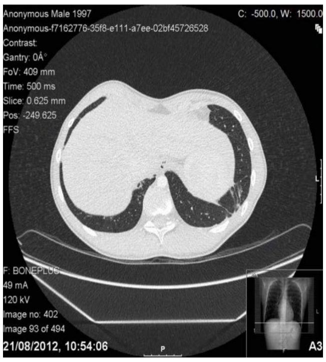

Figure 5. Axial chest CT obtained following chemotherapy and surgery shows a fibrotic scar in the posterior basal segment of the lung.

The description of the local extent of a bone tumor requires X-ray and CT/MRI of the involved bone. A chest CT scan is required to rule out lung or pleural metastases. The screening for bone metastases consists to include 99mTc bone scintigraphy. Many centres are now using FDG-PET scanning or total-body MRI to look for occult metastases. While the role of FDG PET-CT in detecting recurrence is less clear, its role in staging Ewing sarcoma seems to be well established [5]. Other authors state that MRI imaging with Gd enhancement, FDG PET and thallium scan maybe useful for assessment after treatment [6].

Recently, more accurate radiological diagnosis has become possible because of functional examinations such as FDG PET. This case suggests that the importance of recognizing exceptional features when interpreting FDG PET or scintigraphy to prevent the misinterpretation of metastases as perhaps other etiologies, such as infection [7].

Declarations

Conflict of interest

The authors declare that there is no conflict of interest.

References

1.
   Applied to Bone Metastases. Intech open Ed., 2011. p. 339-354, ISBN: 978-953-307-774-1. Available from: www.intechopen.com/books/medical-imaging/advances-in-medical-imaging-applied-to-bone-metastases
2. Foran P, Colleran G, Madewell J, O'Sullivan P. Imaging of thoracic sarcomas of the chest wall, pleura, and lung. Semin Ultrasound CT MR. 2011;32:365-76 pubmed publisher
3. Shamberger R, Laquaglia M, Gebhardt M, Neff J, Tarbell N, Marcus K, *et al*. Ewing sarcoma/primitive neuroectodermal tumor of the chest wall: impact of initial versus delayed resection on tumor margins, survival, and use of radiation therapy. Ann Surg. 2003;238:563-7; discussion 567-8 pubmed
4. Kim S, Lee S, Arsenault D, Strijbosch R, Shamberger R, Puder M. Pediatric rib lesions: a 13-year experience. J Pediatr Surg. 2008;43:1781-5 pubmed publisher
5. Treglia G, Salsano M, Stefanelli A, Mattoli M, Giordano A, Bonomo L. Diagnostic accuracy of ^{1} F-FDG-PET and PET/CT in patients with Ewing sarcoma family tumours: a systematic review and a meta-analysis. Skeletal Radiol. 2012;41:249-56 pubmed publisher
6. Bonakdarpour, A., Reinus, WR. and Khurana JS. Eds. Diagnostic Imaging of Musculoskeletal Diseases. A Systematic Approach. New York, Springer. 2010.
7. Györke T, Zajic T, Lange A, Schäfer O, Moser E, Makó E, *et al*. Impact of FDG PET for staging of Ewing sarcomas and primitive neuroectodermal tumours. Nucl Med Commun. 2006;27:17-24 pubmed

ISSN : 2334-1009